

# Cutting Process Tribometer Experiments for Evaluation of Friction Coefficient close to a CFRP Machining Operation

**Conference Paper****Author(s):**

Voß, Robert; [Seeholzer, Lukas](#) ; Kuster, Friedrich; Wegener, Konrad

**Publication date:**

2017-06

**Permanent link:**

<https://doi.org/10.3929/ethz-b-000165460>

**Rights / license:**

[Creative Commons Attribution-NonCommercial-NoDerivatives 4.0 International](#)

**Originally published in:**

66, <https://doi.org/10.1016/j.procir.2017.03.225>

1<sup>st</sup> CCMPM 2017 – CIRP Conference on Composite Materials Parts Manufacturing

## Cutting Process Tribometer Experiments for Evaluation of Friction Coefficient close to a CFRP Machining Operation

Robert Voss<sup>a,\*</sup>, Lukas Seeholzer<sup>a</sup>, Friedrich Kuster<sup>a</sup>, Konrad Wegener<sup>a</sup><sup>a</sup> Institute of Machine Tools and Manufacturing (IWF), ETH Zurich, Leonhardstrasse 21, 8092 Zurich, Switzerland\* Corresponding author. Tel.: +41 44 6320731 ; fax: +41 446320731. E-mail address: [voss@iwf.mavt.ethz.ch](mailto:voss@iwf.mavt.ethz.ch)

### Abstract

Finishing operations of Carbon Fibre Reinforced Polymers (CFRP), such as drilling or milling are known to generate heavy tool wear. Consequently, ultra-hard cutting materials like diamond-coated carbide tools or PCD-tools are utilised. To further improve the lifetime of these tools, it is recommended to adjust the tool geometry, process parameters and coating to the relevant application. Usually, the process optimisations base on knowledge from fundamental experiments in similar materials or rarely on tool wear modelling. To improve suitable force and tool wear models, the friction coefficients between tool and workpiece under realistic conditions are required.

To address the lack of friction coefficient at the tool/workpiece interface, a cutting process tribometer (CP-T) is utilised. This tribometer enables for friction measurements between diamond-coated cemented carbide pins and freshly generated CFRP surfaces downstream of a orthogonal cutting process. The tribological conditions in the measurement setup (e.g. velocity, pressure and presence of loose particles) are very similar to those occurring at the tool/workpiece interface during the cutting process. It is shown that the magnitude of friction coefficient as well as the influence of the fibre orientation is much lower compared to results of pin-on-disk tribometer (POD-T) experiments. This measurement data is of high relevance for machining force and wear modelling as well as cutting process optimisation.

© 2017 The Authors. Published by Elsevier B.V. This is an open access article under the CC BY-NC-ND license (<http://creativecommons.org/licenses/by-nc-nd/4.0/>).

Peer-review under responsibility of the scientific committee of the 1st Cirp Conference on Composite Materials Parts Manufacturing

**Keywords:** Friction; Diamond Coating; Cutting Operation; Fiber reinforced plastic

### 1. Introduction

Carbon fibre reinforced polymer (CFRP) is currently the most commonly used material in modern airplanes, like the Airbus A350 or the Boeing 787 which are made of about 50% CFRP by weight [1, 2]. Machining of CFRP with high fibre content by drilling or milling is challenging due to the high abrasiveness of the carbon fibres and the heavy wear of the drilling tools, inter alia shown by FERREIRA et al. [3]. The heavy tool wear in turn facilitates generation of damages in the CFRP by the machining process, like delamination or uncut fibres, making manual rework and frequent tool exchanges necessary. Research yields towards optimization of tool geometry and utilization of ultra-hard diamond materials, which are more resistant to abrasive wear: It is state of the art in CFRP machining to use PCD diamond or diamond coated

cemented carbide tools to reach a sufficient tool lifetime, as stated by TETI [4] and HENERICHS et al. [5]. Especially since the coating adhesion of CVD-diamond layers has been improved, in the meantime drastically increased tool lifetimes even for complex tool geometries are possible, as experimentally shown by SUN et al. [6] and HENERICHS et al. [5].

### 2. Initial Situation

Simulation of machining processes, including forces, quality and tool wear is a central research topic not only in machining metals, but also in CFRP machining where the material has anisotropic and inhomogeneous properties. For realistic modelling of CFRP machining processes the understanding of friction and determination of friction

coefficients is required. Due to the anisotropy, fundamental contact theories like the *Hertzian* are not valid for fibre reinforced polymers (FRPs), as stated by NING and LOVELL [7]. HWU and FAN [8, 9] were the first ones deriving a closed-form solution for a sliding contact between bodies and a plane with CFRP properties (elastic, anisotropic) by applying the STROH's formalism [10] for anisotropic elasticity. This approach was used by NING and LOVELL [7] to model sliding friction with FRPs: The authors analysed the influence of the fibre-volume fraction, -orientation, -material, matrix material and friction coefficient on the wear of the FRPs. According to their calculations the friction coefficient has a significant influence on the contact patch for transverse and normal sliding, relative to the fibre direction. While some of the first FEM analyses in FRPs [11-13] neglect friction effects, others [14, 15] use constant coefficients of friction of  $\mu=0.3$  or  $\mu=0.4$  at the flank-face material contact. These friction coefficients are based on measurements by SUNG and SUH [16], shown in Fig. 1 (A), who tested various fibre orientations of graphite-epoxy FRP sliding against 52100 steel. A pin-on-ring apparatus was utilized to test with different speeds and varying fibre orientations relative to the sliding orientation. Normal orientation of the fibres to the sliding surface shows smaller frictional resistance than transverse orientation. NAYAK and BHATNAGAR [17] conducted pin-on-disk experiments with variable fibre orientations of GFRP sliding on HSS under a high normal load of 120 N to determine the directional friction coefficient, shown in Fig. 1 (B). This high normal load is more similar to the machining conditions and promises for more accurate simulation results of a machining operation. But this comparably high load is focused on a rather large theoretical area of 100 mm<sup>2</sup> resulting in just 1.2 MPa. It needs to be considered that the two studies [16, 17] use contrary definition of fibre orientation with respect to the sliding direction, shown in the boxes below the diagrams in Fig. 1. Mismatching the results from Sung and Suh the friction coefficient in Fig. 1 (B) increased from  $\mu=0.3$  at  $\theta=0^\circ$  (transverse) to  $\mu=0.88$  at  $\theta=90^\circ$  (normal), which implies that the normal fibre orientation with respect to the sliding surface has higher frictional resistance. Considering this directional data, the cutting force in NAYAK and BHATNAGAR's [17] macro-mechanical model fits well, but the thrust force shows large variations compared to measurements and even a different trend arises.

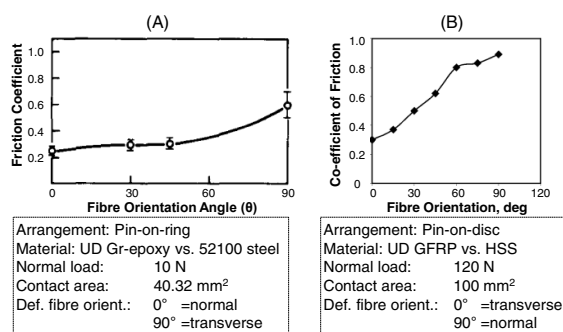


Fig. 1. Friction coefficient according to SUNG and SUH [16] (A) and NAYAK and BHATNAGAR [17] (B).

In the past the friction coefficient between any material and FRP was determined by pin-on-disk, disk-on-disk or other similar closed tribometers, which allow for precise but limited adjustment of the boundary conditions. These setups enable for fast operation with good repeatability under lab conditions but show a multiple sliding contact along the same track, causing run-in effects. As pointed out by MONDELIN et al. [18] and PULS et al. [19], such closed tribometers neither reflect machining contact conditions nor use freshly generated surfaces for the sliding contact, as being typical for machining with continuous material flow along the tool faces. To date very few studies [18, 20, 21] exist, focusing on the determination of friction coefficient between CFRP and diamond under realistic cutting conditions:

- MONDELIN et al. [18] present the friction coefficient between monocrystalline diamond and CFRP dependent on various contact pressures, sliding velocities (20 m/min and 40 m/min), CFRP layer orientations and consider utilization of cutting fluid. The experimental friction coefficients for CFRP-Diamond are significantly smaller than any other value reported in literature and vary between 0.08 to 0.12 for dry and 0.06 to 0.07 for lubrication conditions. Due to the CFRP probe shape (sheet material) and unavailability of unidirectional material, the influence of fibre orientation has not been analysed.
- WANG et al. [20] determine the temperature influence on the friction coefficient between carbon/epoxy composites and monocrystalline diamond. The sliding speed over the unidirectional CFRP sheet material was just 0.5 m/min. The authors measure a coefficient of friction of  $\mu=0.125$  for sliding in fibre orientation ( $0^\circ$ ) and  $\mu=0.175$  for sliding perpendicular ( $90^\circ$ ). With increasing temperature the friction coefficient increases to  $\mu=0.4$  at  $125^\circ\text{C}$  and drastically decreases when exceeding the glass transition temperature, due to changes in the epoxy resin properties.
- CHARDON et al. [21] analyse the influence of high sliding velocities (up to 800 m/min) on the friction coefficient between polycrystalline diamond (PCD) and randomly structured CFRP. In general the friction coefficients with values between  $\mu=0.05$  and  $\mu=0.08$  are even lower than those obtained between monocrystalline diamond and CFRP in [18]. It needs to be considered that different CFRP materials were tested in these studies. For high speeds ( $>100$  m/min) the influence of the sliding velocity on the friction coefficient seems to be low.

The goal of this study is to address the lack of friction coefficient between CVD-diamond and CFRP under realistic cutting conditions with an open cutting process tribometer (CP-T), which enables for friction measurements close to the machining process. This CP-T is based on an orthogonal cutting process with a spring pre-loaded pin sliding downstream, but close to the process, on the freshly generated material surface. The process enables testing of various fibre orientations, relative to the sliding direction.

### 3. Experimental Approach

The experimental setup for the turning tests is carried out on an Okuma LB15-II lathe. With experiments in titanium, presented by SMOLENICKI et al. [22], the CP-T setup showed its capability and is now adapted to determine the friction coefficient between heterogeneous CFRP and CVD-diamond. It has been arranged to allow machining CFRP in an orthogonal turning operation at constant fibre orientation  $\theta$ . Figure 2 (A) shows exemplary manufacturing of the unidirectional semi-circular shaped CFRP laminate with constant fibre orientation of  $\theta=45^\circ$ .

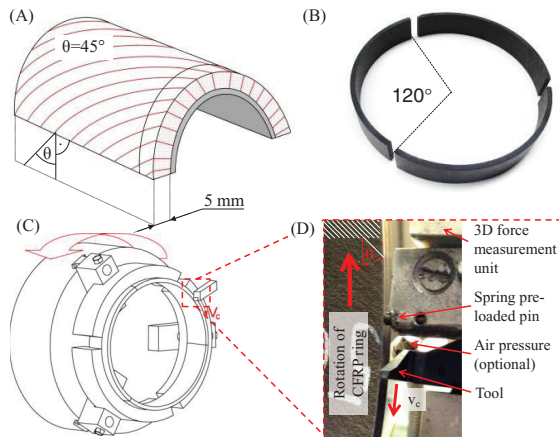


Fig. 2. (A) CFRP workpiece with exemplary fibre orientation  $\theta=45^\circ$ ; (B) CFRP segments prior to machining; (C) schematic illustration of ring-shaped workpieces clamped into machine tool as in [23] and (D) detailed view of contact conditions during machining.

By means of waterjet machining three segments of each 120° are cut out and may be assembled to a ring. In Fig. 2 (C) and (D) the CFRP segments are presented clamped into the chuck of the lathe. The diameter of the CFRP ring is 200 mm and the CFRP width is 5 mm.

#### 3.1. Cutting Tools and Pins

Conventional carbide cutting inserts of the grade MG12 (Ceratizit) with nano-crystalline CVD-diamond coating of  $8^{+2} \mu\text{m}$  thickness are utilized. Three different tool geometries with varying rake and clearance angles are generated by grinding: RA with  $\gamma=0^\circ$  and  $\alpha=14^\circ$ ; RB with  $\gamma=20^\circ$  and  $\alpha=14^\circ$ ; RC with  $\gamma=20^\circ$  and  $\alpha=7^\circ$ . The cutting edge radius in the new state of the CVD-coated tools is  $\sim 18 \mu\text{m}$ .

Carbide pins of the same grade (MG12) and with the same CVD-coating (Diamond Nano Plus  $8^{+2} \mu\text{m}$ ) as the cutting inserts are generated to slide on the freshly generated CFRP surface. The diameter of the cylindrical pins, which are marked red in Fig. 3, is 3 mm and the overall length is 17 mm. One side of the pin, which slides on the CFRP surface, has a spherical shape of 3 mm radius.

#### 3.2. Material Properties

Unidirectional CFRP M21/34%/UD194/IMA-12K is utilized for the experiments, as in the study [23] presented at HPC 2014. This material is common in the aerospace industry. It contains 66% (by weight) intermediate modulus (IM) carbon fibres and high performance matrix material HexPly® M21 [Hexcel]. The material is well known to be difficult to machine. Both, the high fibre content as well as the high toughness of the fibre and matrix system cause extensive tool wear. Drilling operations of this material result in serious delamination due to the unidirectional configuration and the difficult cutting characteristics of the fibre. The material properties of the CFRP with epoxy matrix material are presented in Table 1. Six fibre orientations are tested:  $\theta=0^\circ$ ,  $30^\circ$ ,  $60^\circ$ ,  $90^\circ$ ,  $120^\circ$ ,  $150^\circ$ .

Table 1. Physical and mechanical properties of IMA-12K fibres

Physical properties	Fibre	Weave/UD	Fibre Mass [g/m <sup>2</sup> ]	Fibre volume [%]	Laminate Density [g/cm <sup>3</sup> ]	Glass Trans. Temp. [°C]
	IMA	UD	194	59.2	1.58	195
Mech. properties	Tensile	Tensile strength [MPa]	Tensile modulus [GPa]	Compression	Compr. Strength [MPa]	Compr. Modulus [GPa]
	Method EN6032	3050	178	Method EN2561 B	1500	146

#### 3.3. Cutting Process Tribometer

To ensure contact conditions between CFRP surface and the CVD-diamond coated pin being as similar to the cutting process as possible, the pin is situated only 14 mm behind the cutting edge. In this way, the cutting velocity of the infinite, non-interrupted cut and sliding velocity correspond. At an exemplary cutting speed of  $v_c=100 \text{ m/min}$ , the time interval from the cutting edge to the pin is 8.4 ms. This leads to the assumption that the temperature at the CFRP surface at sliding position is still similar to the one during CFRP cutting. Furthermore high-speed camera images proof the existence of loose CFRP and matrix particles floating close to the CFRP surface at pin position.

These particles were forced underneath the cutting edge during the machining process instead of being evacuated along the rake face of the tool. The normal load between pin and CFRP surface is set to the actual forces occurring in the orthogonal cutting process, measured during separate experiments (range  $\sim 50 \text{ N} - 200 \text{ N}$ ). This setting close to a machining operation promises to measure the friction coefficient at the pin under similar conditions (speed, temperature, normal load, existence of loose particles), as prevail along the tool flank face during machining.

The setup enables evaluation of variable fibre orientation by changing the direction ( $\theta$ ) of laminate in the semi-circular shaped raw material in Fig. 2. The aforementioned experiments by SUNG et al. [16] and NAYAK and BHATNAGAR [17] with HSS tools at low sliding velocities suggest a strong dependency of the friction coefficient on the fibre orientation.

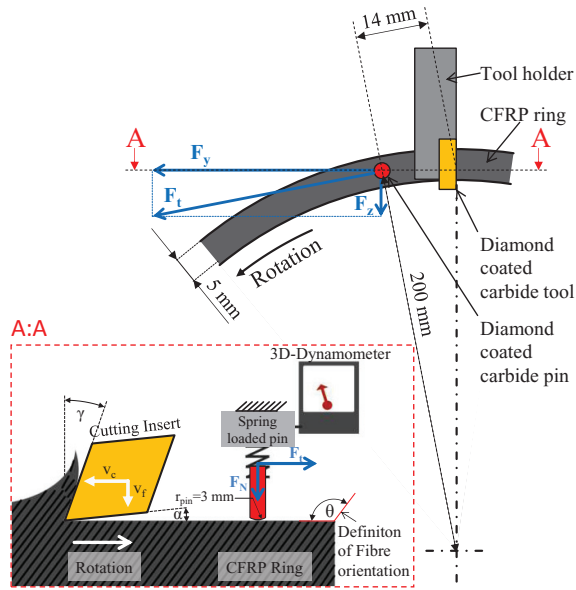


Fig. 3. Scheme and geometrical conditions of the cutting process Tribometer (CP-T).

Friction forces and normal load on the pin are measured with a 3D-dynamometer 9047C by Kistler. According to the geometrical conditions, shown in Fig. 3, the friction force  $F_t$  is calculated as the resulting force composed by  $F_y$  and  $F_z$ .

$$F_t = \sqrt{F_y^2 + F_z^2} \quad (1)$$

The apparent friction coefficient  $\mu_{app}$  is provided by the ratio between friction force  $F_t$  and the normal force  $F_N$ , measured as average value in the stable machining zone. According to MONDELIN et al. [18], who refers to the analytical solution developed by LAFAYE et al. [24, 25], the apparent friction coefficient  $\mu_{app}$  represents a superposition of adhesion and plastic deformation effects, as illustrated in Fig. 4.

$$\mu_{app} = \frac{F_t}{F_N} = \mu_{adh} + \mu_{def} \quad (2)$$

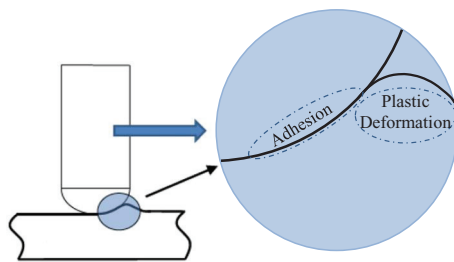


Fig. 4. Illustration of plastic deformation and adhesion in friction tests, according to MONDELIN et al. [18].

### 3.4. Experimental Procedure

The unidirectional CFRP is machined in an orthogonal turning process. The machining conditions are constant during one experiment. But within the experimental series variable tool geometries, fibre orientations, feed rates and cutting velocities are tested, presented in Table 2. All experiments are conducted under dry cutting conditions. A new diamond coated pin is used for each separate experiment. One CP-T experiment is completed as soon a feed path of 2 mm is incrementally machined, which takes about 67 rotations at a feed rate  $f=0.03$  mm. The cutting width is  $a_c=5$  mm which is equal to the wall thickness, resulting in full section cuts.

Table 2. Machining parameters of orthogonal turning tests.

$\gamma; \alpha$ [deg]	$v_c$ [m/min]	$f$ [mm]	$a_c$ [mm]	$\theta$ [deg]
0, 20; 7, 14	60, 90	0.03, 0.06, 0.1	5	0, 30, 60, 90, 120, 150

### 4. Results and Discussion

Figure 5 shows the influence of a variable fibre cutting angle on the apparent friction coefficient. In contrast to experiments [16, 17] with closed tribometers (pin-on-disk, etc.) and steel sliding on CFRP/epoxy, presented in Fig. 1, in the experiments with the introduced setup the fibre orientation has a lower influence: The measurement values range between  $\mu_{app}=0.11$  and  $\mu_{app}=0.15$  and are slightly larger compared to MONDELIN et al. [18] with monocrystalline diamond ( $0.08 < \mu_{app} < 0.12$ ). Maximum values appear for  $\theta=0^\circ=180^\circ$  (parallel) and  $\theta=90^\circ$  (normal), while  $\theta=30^\circ$  and  $\theta=150^\circ$  generate somewhat smaller values ( $\mu_{app}=0.12$ ). Each tested fibre orientation is averaged at least on three measurements. In contradiction to the results of SUNG and SUH [16] and NAYAK and BHATNAGAR [17] the pronounced effect of fibre orientation on the friction coefficient cannot be confirmed. According to analyses by MATSUNAGA et al. [26], pronounced effects of fibre orientation on the friction coefficient are somewhat suppressed for higher contact pressures as they occur in cutting: Based on measurements of the pin-track width on the CFRP surface, a contact area of  $0.265\text{--}2.14\text{ mm}^2$  occurs in this experiments depending on the normal load and fibre orientation. It results in average contact pressures of 90–530 MPa. Furthermore the presence of loose CFRP and matrix particles, partly covering the freshly generated CFRP surface, might change the friction process from mainly sliding to rolling and reduce the influence of fibre orientation in the sliding contact.

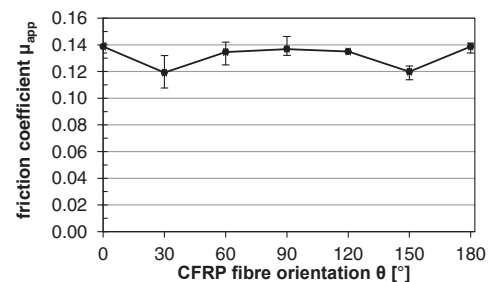


Fig. 5. Influence of fibre cutting angle  $\theta$  on the apparent friction coefficient.



Analysing the apparent friction coefficients from Fig. 5 in detail, the data is plotted over the normal pin pre-load in Fig. 6. It does not show an explicit trend: While for fibre orientations of  $\theta=30^\circ$  and  $\theta=60^\circ$  a slightly increasing trend with increasing load is visible, for the other orientations superimposing scattering effects prevent an explicit conclusion. These observations are in accordance with results reported by MONDELIN et al. [18] that contact pressure does not significantly influence the friction coefficient between CFRP and diamond.

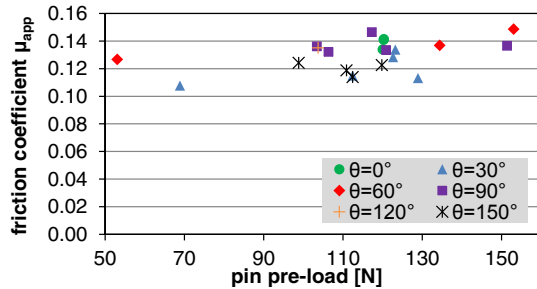


Fig. 6. Influence of pin pre-load on the apparent friction coefficient.

As presented by HENERICHS and VOSS et al. [23, 27, 28], the fibre orientation of  $\theta=150^\circ$  leads to saw tooth like surface topography, shown in Fig. 7. Accordingly, the feed rate and slightly the rake angle  $\gamma$  influence the generated tooth size  $L_z$  for  $\theta=150^\circ$ . The larger  $L_z$ , the higher the roughness. It is well known that the surface roughness value  $R_a$  is not sufficient in CFRP machining, thus  $\mu_{app}$  is compared to  $R_z$  (av. of peak-to-valley distance) and  $R_p$  (maximum peak height) in Fig. 7.

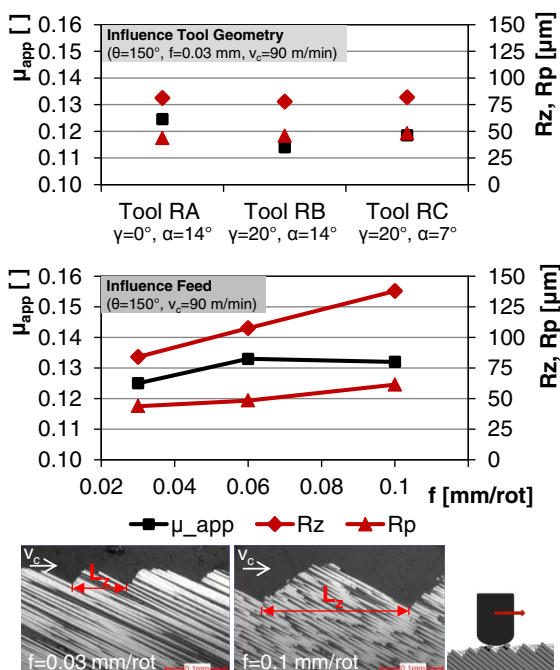


Fig. 7. Influence of tool geometry and feed rate on roughness and friction coefficient for  $\theta=150^\circ$ .

Interestingly, no generally valid correlation between surface roughness and apparent friction coefficient could be found for  $\theta=150^\circ$ . Only for smallest saw teeth ( $f=0.03$  mm/rot),  $\mu_{app}$  is slightly reduced, which might be due to less plastic deformation ahead of the spherical shaped pin. For the other tested fibre orientations ( $\theta \neq 150^\circ$ ), the influence of the tool geometry on  $\mu_{app}$  is not significant.

## 5. Conclusion

The presented tribometer experiments close to the machining process confirm the results of MONDELIN et al. [18], WANG et al. [20] and CHARDON et al. [21], that the apparent friction coefficient between CFRP and diamond is lower than any other reported friction coefficient in CFRP literature: A range of  $0.11 \leq \mu_{app} \leq 0.15$  occurs.

The cutting process tribometer setup has been newly developed to enable evaluation of the CFRP fibre orientation on the friction coefficient. Laminates with parallel ( $\theta=0^\circ$ ) and perpendicular orientation ( $\theta=90^\circ$ ) of the carbon fibres relative to the cutting velocity result in similar values of  $\mu_{app}=0.14$ , whereas orientations of  $\theta=30^\circ$  and  $\theta=150^\circ$  show slightly lower values of  $\mu_{app}=0.12$ . In general the presented setup close to the machining process shows a weaker dependency of the friction coefficient on the fibre orientation compared to aforementioned publications with steel and CFRP as friction partners. This effect might be due to the following reasons:

- Loose CFRP and fibre particles from the machining operation cover the freshly generated surface and result rather in a rolling layer than in sliding effects
- High, machining-like stresses at CFRP-pin contact suppress the effects of fibre orientation

Experiments with variable pin pre-load confirm former findings and show no significant influence of the load on the friction coefficient. Tests with  $\theta=150^\circ$  fibre orientation show particular results because this fibre orientation tends to generate a saw tooth topography depending on the tool rake angle and feed rate: The larger the feed, the larger the saw teeth which is proportional to the roughness. The smallest feed rate ( $f=0.03$  mm/rot) results in the lowest frictional resistance when sliding with a pin over such a topography.

In general the utilized tribometer setup close to an orthogonal cutting operation shows its suitability even for machining of inhomogeneous CFRP material.

## Acknowledgements

The authors thank the Commission for Technology and Innovation (CTI Project 15093.1 PFIW-IW), the companies Dixi Polytool SA, Heule Werkzeug AG, Oerlikon Balzers AG and RUAG Switzerland AG for the support.

## References

- [1] Kraus T and Kühnel M. Der globale CFK-Markt. *Composites Marktbericht 2015*; Last update: 2015 [cited 01.01.2016]; Available from: <http://www.avk->

- tv.de/files/20151214\_20150923\_composites\_marktb  
ericht\_gesamt.pdf.
- [2] Sheikh-Ahmad J Y. *Machining of Polymer Composites*. Abu Dhabi, United Arab Emirates: Springer-Verlag; 2009.
- [3] Ferreira J, Coppini N, and Miranda G. Machining optimisation in carbon fibre reinforced composite materials. *Journal of materials processing technology*; 1999. **92**: p. 135-140.
- [4] Teti R. Machining of Composite Materials. *CIRP Annals - Manufacturing Technology*; 2002. **51**(2): p. 611-634.
- [5] Henerichs M, Dold C, Voss R, and Wegener K. Performance of Lasered PCD-and CVD-Diamond Cutting Inserts for Machining Carbon Fiber Reinforced Plastics (CFRP). in *Int. Mechanical Engineering Congress and Exposition*; 2013. San Diego, California (USA): American Society of Mechanical Engineers (ASME).
- [6] Sun F, Zhang Z, Chen M, and Shen H. Fabrication and application of high quality diamond-coated tools. *Journal of materials processing technology*; 2002. **129**(1): p. 435-440.
- [7] Ning X and Lovell M R. On the sliding friction characteristics of unidirectional continuous FRP composites. *Journal of tribology*; 2002. **124**(1): p. 5-13.
- [8] Hwu C and Fan C. Contact problems of two dissimilar anisotropic elastic bodies. *Journal of applied mechanics*; 1998. **65**(3): p. 580-587.
- [9] Hwu C and Fan C. Sliding punches with or without friction along the surface of an anisotropic elastic half-plane. *The Quarterly Journal of Mechanics and Applied Mathematics*; 1998. **51**(1): p. 159-177.
- [10] Stroh A N. Dislocations and cracks in anisotropic elasticity. *Philosophical magazine*; 1958. **3**(30): p. 625-646.
- [11] Ramesh M, Seetharamu K, Ganesan N, and Sivakumar M. Analysis of machining of FRPs using FEM. *International Journal of Machine Tools and Manufacture*; 1998. **38**(12): p. 1531-1549.
- [12] Mahdi M and Zhang L. An adaptive three-dimensional finite element algorithm for the orthogonal cutting of composite materials. *Journal of Materials Processing Technology*; 2001. **113**(1): p. 368-372.
- [13] Mahdi M and Zhang L. A finite element model for the orthogonal cutting of fiber-reinforced composite materials. *Journal of Materials Processing Technology*; 2001. **113**(1): p. 373-377.
- [14] Arola D and Ramulu M. Orthogonal cutting of fiber-reinforced composites: a finite element analysis. *International journal of mechanical sciences*; 1997. **39**(5): p. 597-613.
- [15] Arola D, Sultan M B, and Ramulu M. Finite element modeling of edge trimming fiber reinforced plastics. *Journal of manufacturing science and engineering*; 2002. **124**(1): p. 32-41.
- [16] Sung N-H and Suh N P. Effect of fiber orientation on friction and wear of fiber reinforced polymeric composites. *Wear*; 1979. **53**(1): p. 129-141.
- [17] Nayak D, Bhatnagar N, and Mahajan P. Machining studies of UD-FRP composites part 2: finite element analysis. *Machining Science and Technology*; 2005. **9**(4): p. 503-528.
- [18] Mondelin A, Furet B, and Rech J. Characterisation of friction properties between a laminated carbon fibres reinforced polymer and a monocrystalline diamond under dry or lubricated conditions. *Tribology International*; 2010. **43**(9): p. 1665-1673.
- [19] Puls H, Klocke F, and Lung D. A new experimental methodology to analyse the friction behaviour at the tool-chip interface in metal cutting. *Production engineering*; 2012. **6**(4-5): p. 349-354.
- [20] Wang B, Gao H, Zhang S P, and Bao Y J. Study on friction coefficient between carbon/epoxy composites and a monocrystalline diamond under different temperatures. in *Advanced Materials Research*; 2012. Trans Tech Publ.
- [21] Chardon G, Klinkova O, Rech J, Drapier S, and Bergheau J-M. Characterization of friction properties at the work material/cutting tool interface during the machining of randomly structured carbon fibers reinforced polymer with Poly Crystalline Diamond tool under dry conditions. *Tribology International*; 2015. **81**: p. 300-308.
- [22] Smolenicki D, Boos J, Kuster F, Roelofs H, and Wyen C. In-process measurement of friction coefficient in orthogonal cutting. *CIRP Annals-Manufacturing Technology*; 2014. **63**(1): p. 97-100.
- [23] Voss R, Henerichs M, Kuster F, and Wegener K. Chip root analysis after machining carbon fiber reinforced plastics (CFRP) at different fiber orientations. in *CIRP HPC*; 2014: Berkeley (US). p. 217-222.
- [24] Lafaye S, Gauthier C, and Schirrer R. The ploughing friction: analytical model with elastic recovery for a conical tip with a blunted spherical extremity. *Tribology Letters*; 2006. **21**(2): p. 95-99.
- [25] Lafaye S, Gauthier C, and Schirrer R. A surface flow line model of a scratching tip: apparent and true local friction coefficients. *Tribology international*; 2005. **38**(2): p. 113-127.
- [26] Matsunaga S, Matsubara T, Wang W-X, and Takao Y. Effects of reciprocation number on the friction behaviors of carbon/epoxy for various fiber orientations and high contact pressures. Int. Conference on Composite Materials (ICCM). 2001. **13**, DOI: ID 1446.
- [27] Henerichs M, Voss R, Kuster F, and Wegener K. Machining of carbon fiber reinforced plastics: Influence of tool geometry and fiber orientation on the machining forces. *CIRP Journal of Manufacturing Science and Technology*; 2015. **9**: p. 136-145.
- [28] Henerichs M, Bohrbearbeitung von CFK unter besonderer Berücksichtigung der Schneidkantenmikrogeometrie. 2015, Eidgenössische Technische Hochschule Zürich (ETH), Nr. 22629: Zürich.